# Section 2

# Data sets, diagnostic and dynamical investigations, statistical post-processing , multi-year reanalyses and associated studies

# Cumulonimbus clouds and thunderstorms in summer over Russia: Changes during 1966-2010

Chernokulsky A.V., Mokhov I.I.
A.M. Obukhov Institute of Atmospheric Physics RAS
a.chernokulsky@ifaran.ru

Recent studies show the increase of the forest fires risk in Northern Eurasia regions under expected climate changes [Mokhov et al., 2006; Mokhov and Chernokulsky, 2010; Groisman et al., 2012]. Significant part (about 15-20%) of forest fires is initiated by lightning. Here, we assess the changes in the occurrence of Cumulonimbus clouds (CbO) and thunderstorms (ThO) in summer over Russia from routine 3-hourly synoptic observations on meteorological stations during 1966-2010 [Chernokulsky et al., 2011].

We found that total cloud fraction in summer has a positive trend over Russia as a whole (about 2-4%/decade) due to an increase of CbO with an occurrence of high-level cloudiness (cirrus form). However, changes of low cloud fraction (cumuli and strati) vary significantly from station to station. The CbO has positive trend up to 6-8%/decade for many Russian stations (Fig. 1). Other low-level cloud types (Cumulus, Nimbostratus and Stratus) display domination of negative values for trends (3-5%/decade for cumuli and 1-3%/decade for strati) with minor regional exceptions. In particular, an increase of the occurrence for stratus clouds is noted over the coastal regions of the Far East (about 4-7%/decade). In general, the occurrence of convective clouds tends to increase with more intensive cumuli, the occurrence of stratiform clouds tends to decrease.

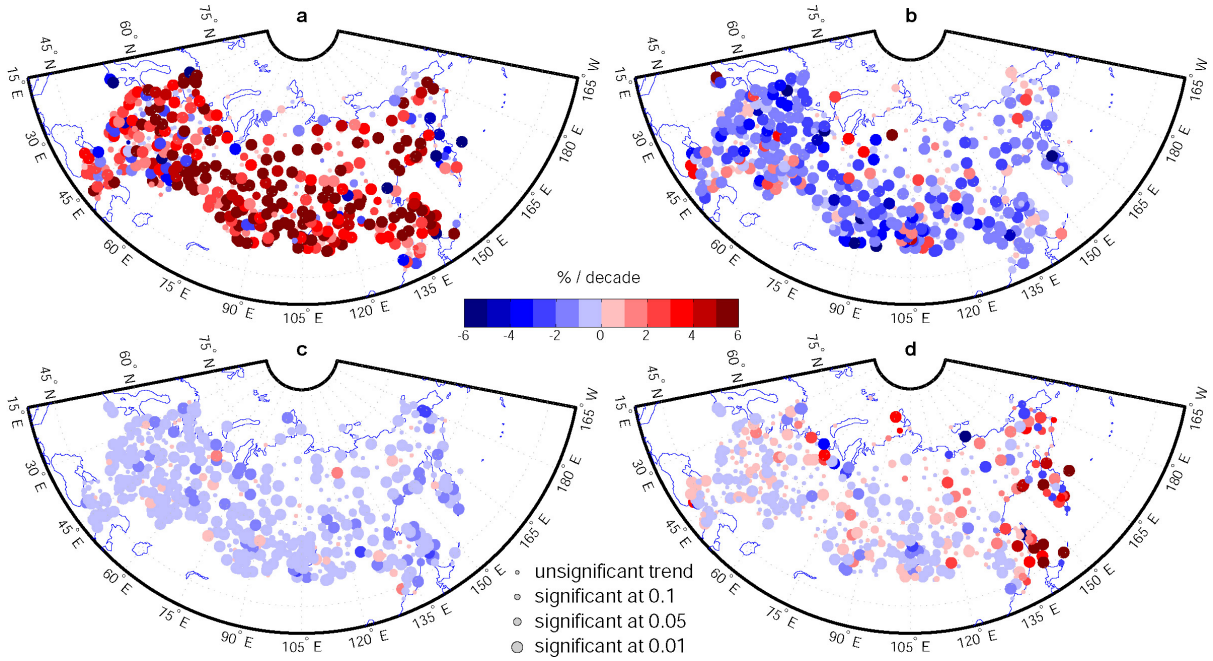


Figure 1. Trends of the occurrence of reports with Cumulonimbus clouds (a), Cumulus clouds (b), Nimbostratus clouds (c) and Stratus clouds (d) in summer during 1966-2010.

An increase of CbO can lead to an increase of the thunderstorm events occurrence (ThO). Coefficient of linear regression *r* of ThO to CbO in summer varies between 0.1 to 0.3 (with the maximum over Caucasus and south of Ural) (Fig.2a). Coefficient *r* is maximal in July-January (Fig.2b) (up to 0.45 for the entire Caucasus region). An increase of *r* from the first period (1966-1987) to the second one (1989-2010) is revealed. Moreover, statistical significance of *r* is increased from the first period to the second one as well. This comes from the

change in sign for ThO trends (from negative to positive, except Caucasus with positive trend for both periods) (Fig. 3).

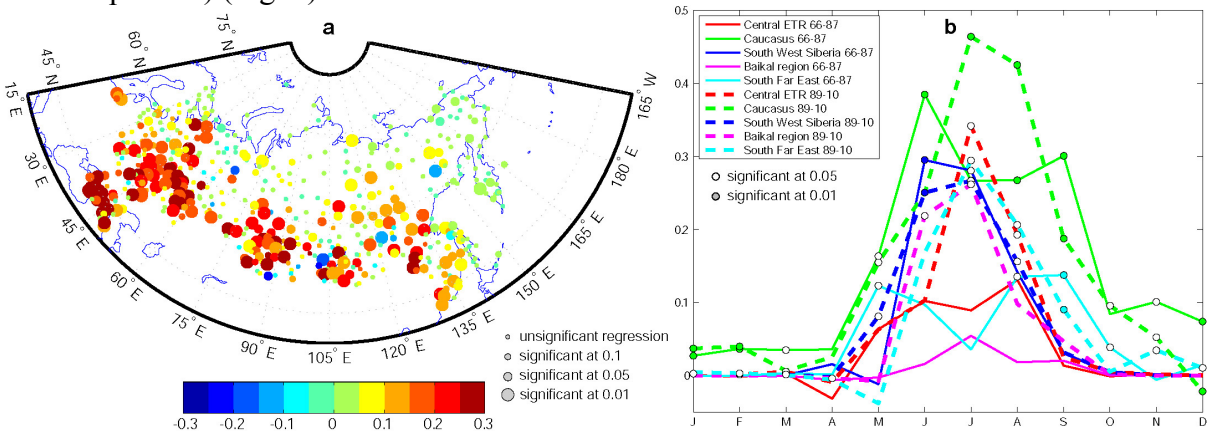


Figure 2. Coefficient of linear regression *r* for the occurrence of days with thunderstorms to the occurrence of days with Cumulonimbus clouds: spatial distribution for r in summer for the period 1966-2010 (a) and annual cycles for two 22-years periods (1966-1987 and 1989-2010) (b) for: 1. Central region of the European part of Russia (50N-60N, 30E-60E), 2. Caucasus region (40N-50N, 35E-50E), 3. South-west of Siberia (50N-60N, 65E-95E), 4. Baikal region (50N-60N, 105E-120E), and 5. South of the Far East (40N-55N, 125E-140E).

In general, cloudiness changes over Russia during last decades point to an increase of the fire ignition risk in summer. This tendency together with an increase of weather-associated fire indices should lead to more fire-hazardous regional climate in Northern Eurasia.

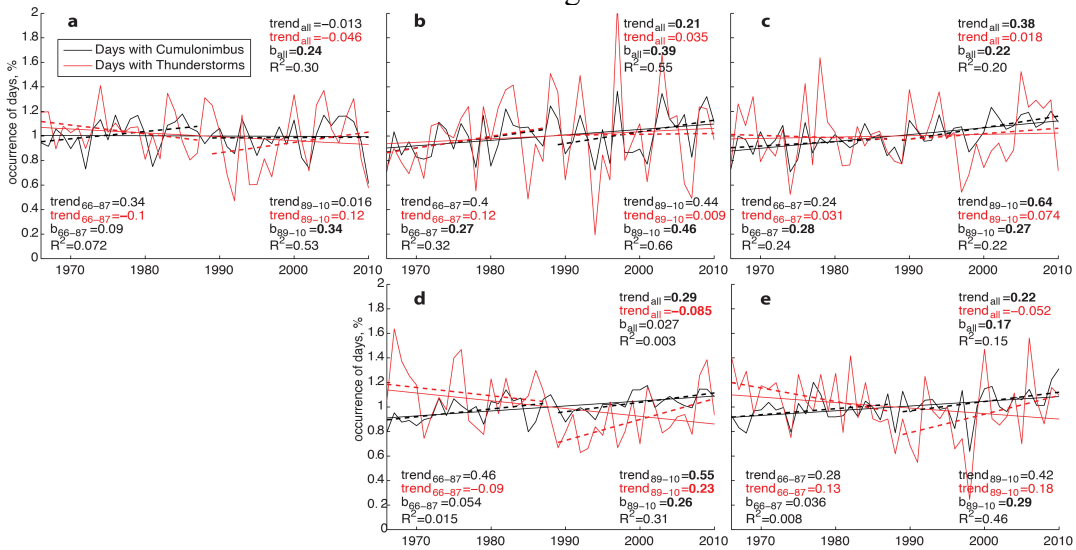


Figure 3. Interannual variations in the number of days in July with CbO and ThO for different regions (see caption to Fig.2). Coefficients of CbO and ThO trends, coefficient of linear regression of ThO to CbO and corresponding coefficient of determination are displayed (bold font corresponds to 0.05 confidence level).

**References**


1. Chernokulsky A.V., O.N. Bulygina and I.I. Mokhov, 2011: Recent variations of cloudiness over Russia from surface daytime observations. *Environ. Res. Lett.,* **6**(3), 035202.
2. Groisman P.Ya., T.A. Blyakharchuk, A.V. Chernokulsky et al., 2012: Climate Changes in Siberia. In: Regional Environmental Changes in Siberia and Their Global Consequences. P.Ya. Groisman and G. Gutman (eds.). Dordrecht: Springer, 57-109.
3. Mokhov I.I. and A.V. Chernokulsky, 2010: Regional model assessments of forest fire risks in the Asian part of Russia under climate change. *Geography and Natural Resources*, **31**(2), 165-169.
4. Mokhov I.I., A.V. Chernokulsky and I.M. Shkolnik, 2006: Regional model assessments of fire risk under global climate changes. *Doklady Earth Sci.,* **411A**(9), 1485-1488.

# Comparison of objective frontal analysis schemes using the NCEP reanalysis

Pandora Hope[1], Kevin Keay[1], and Ian Simmonds[2]

[1]Bureau of Meteorology, Melbourne, Victoria 3001, Australia
[2]School of Earth Sciences, The University of Melbourne, Victoria, 3010, Australia
p.hope@bom.gov.au

The objective identification analysis of cyclonic systems is now well established (e.g., Simmonds and Keay 2002, Wernli and Schwierz 2006, Neu et al. 2013). Among the important reasons for studying extratropical cyclones is their intimate association with precipitation (Rudeva and Gulev 2011). In recent times a considerably enhanced effort has gone into the objective analysis of fronts (e.g., Berry et al. 2011, Simmonds et al. 2012). The identification and tracking of fronts is a more difficult than for the case of cyclones, but arguably it offers more insights into synoptic activity and precipitation distribution (Hope et al. 2014).

We are analysing the behaviour of five rather different objective frontal analysis algorithms (based on, respectively, (1) shifts in 850-hPa winds, (2) gradients of temperature, (3) gradients of wet-bulb potential temperature, (4) pattern matching, and (5) a self-organizing map approach. A sixth method used a manual synoptic technique. A focus was on the critical winter period over part of the wheatbelt of southwest Western Australia (Fig. 1) for 1979-2006 using the NCEP-NCAR reanalysis. (Much of the winter rainfall over this region originates from frontal systems.) Most methods identify the same systems for a significant proportion of the time, while their association with rainfall is less clear. As demonstrated in Hope et al. (2014) we can conclude that automated techniques have great value in understanding frontal behaviour and can be used to identify the changes in the frequency of frontal systems through time and their consequences.

***References***

Berry, G., M. J. Reeder and C. Jakob, 2011: A global climatology of atmospheric fronts. *Geophys. Res. Lett.*, **38**, L04809, doi: 10.1029/2010GL046451.

Hope, P., K. Keay, M. Pook, J. Catto, I. Simmonds, G. Mills, P. McIntosh, J. Risbey and G. Berry, 2014: A comparison of automated methods of front recognition for climate studies: A case study in southwest Western Australia. *Mon. Wea. Rev.*, **142**, 343-363, doi: 10.1175/mwr-d-12-00252.1.

Neu, U., M. G. Akperov, N. Bellenbaum, R. Benestad, R. Blender, R. Caballero, A. Cocozza, H. F. Dacre, Y. Feng, K. Fraedrich, J. Grieger, S. Gulev, J. Hanley, T. Hewson, M. Inatsu, K. Keay, S. F. Kew, I. Kindem, G. C. Leckebusch, M. L. R. Liberato, P. Lionello, I. I. Mokhov, J. G. Pinto, C. C. Raible, M. Reale, I. Rudeva, M. Schuster, I. Simmonds, M. Sinclair, M. Sprenger, N. D. Tilinina, I. F. Trigo, S. Ulbrich, U. Ulbrich, X. L. Wang and H. Wernli, 2013: IMILAST: A community effort to intercompare extratropical cyclone detection and tracking algorithms. *Bull. Amer. Meteor. Soc.*, **94**, 529-547, doi: 10.1175/BAMS-D-11-00154.1

Rudeva, I., and S. K. Gulev, 2011: Composite analysis of North Atlantic extratropical cyclones in NCEP-NCAR reanalysis data. *Mon. Wea. Rev.*, **139**, 1419-1446.

Simmonds, I., and K. Keay, 2002: Surface fluxes of momentum and mechanical energy over the North Pacific and North Atlantic Oceans. *Meteor. Atmos. Phys.*, **80**, 1-18.

Simmonds, I., K. Keay and J. A. T. Bye, 2012: Identification and climatology of Southern Hemisphere mobile fronts in a modern reanalysis. *J. Climate*, **25**, 1945-1962, doi: 10.1175/JCLI-D-11-00100.1.

Wernli, H., and C. Schwierz, 2006: Surface cyclones in the ERA-40 dataset (1958-2001). Part I: Novel identification method and global climatology. *J. Atmos. Sci.*, **63**, 2486-2507.

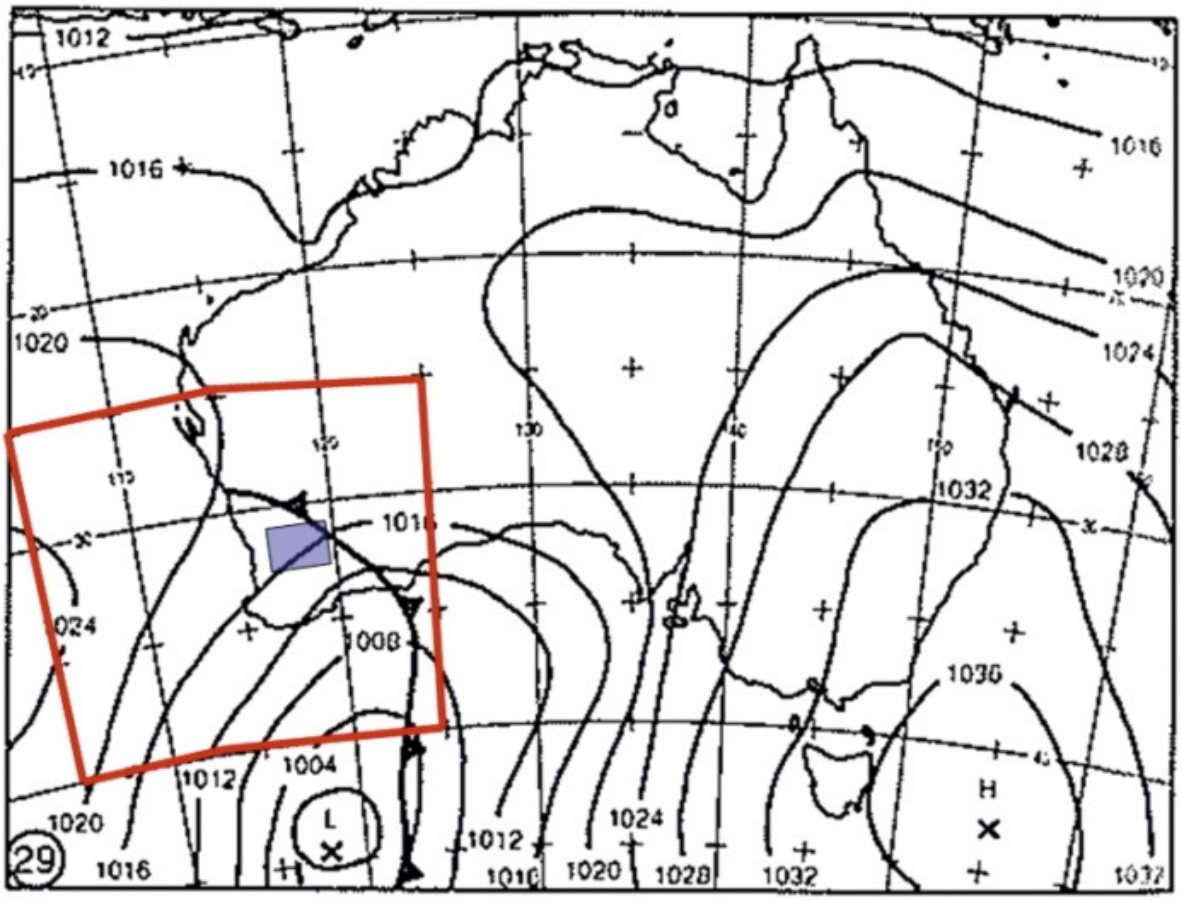


**Figure 1:** **Red** rectangle is region over which fronts are counted, and small **blue** region indicates wheatbelt region investigated here. The synoptic pattern shown is for the strong front of 29 June 1993.

# ATMOSPHERIC EXTRATROPICAL VORTICES: CYCLONE-ANTICYCLONE ASYMMETRY

Mokhov I.I., Akperov M.G., Prokofyeva M.A.

*A.M. Obukhov Institute of Atmospheric Physics RAS, Moscow, Russia*
mokhov@ifaran.ru

Relationships between extratropical cyclones and anticyclones in the Northern Hemisphere are analyzed with the use of the NCEP/NCAR reanalysis data for the period 1948-2012. The characteristics of extratropical cyclones and anticyclones are determined similar to (Akperov et al., 2007; Akperov and Mokhov, 2013).

Figure 1 shows interannual variations for relation ($N_c/N_{ac}$) of the cyclones number $N_c$ to the anticyclones number $N_{ac}$ during 1948-2012 in winter, summer and for annual means. According to Fig. 1 the $N_c/N_{ac}$ relation is larger for summer than that for winter.

Similar cyclone-anticyclone asymmetry is characteristic for the total duration of extratropical cyclones $(N\tau)_c$ and anticyclones $(N\tau)_{ac}$.or for their frequency (see also Mokhov et al., 1992)

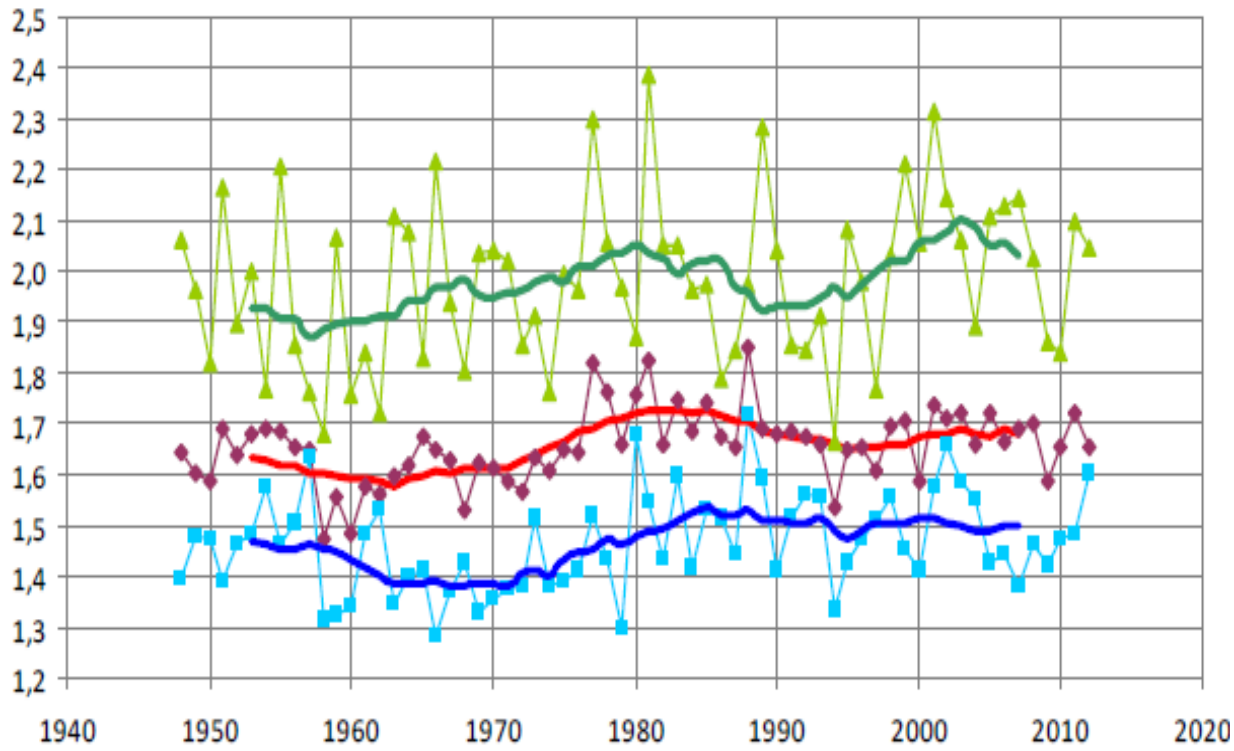


Figure 1. Interannual variations for relation of the cyclones number to the anticyclones number during 1948-2012 in winter (blue curves), summer (green curves) and for annual means (red curves). Bold curves are corresponding variations with the 11-years moving averaging.

Figure 2 illustrates the relationship between the annual-mean total duration of extratropical cyclones $(N\tau)_c$ and anticyclones $(N\tau)_{ac}$ with different life times (from 1 day to 13 days) obtained from reanalysis data for two periods (1948-1977 and 1983-2012). Similar dependencies were obtained for different seasons.

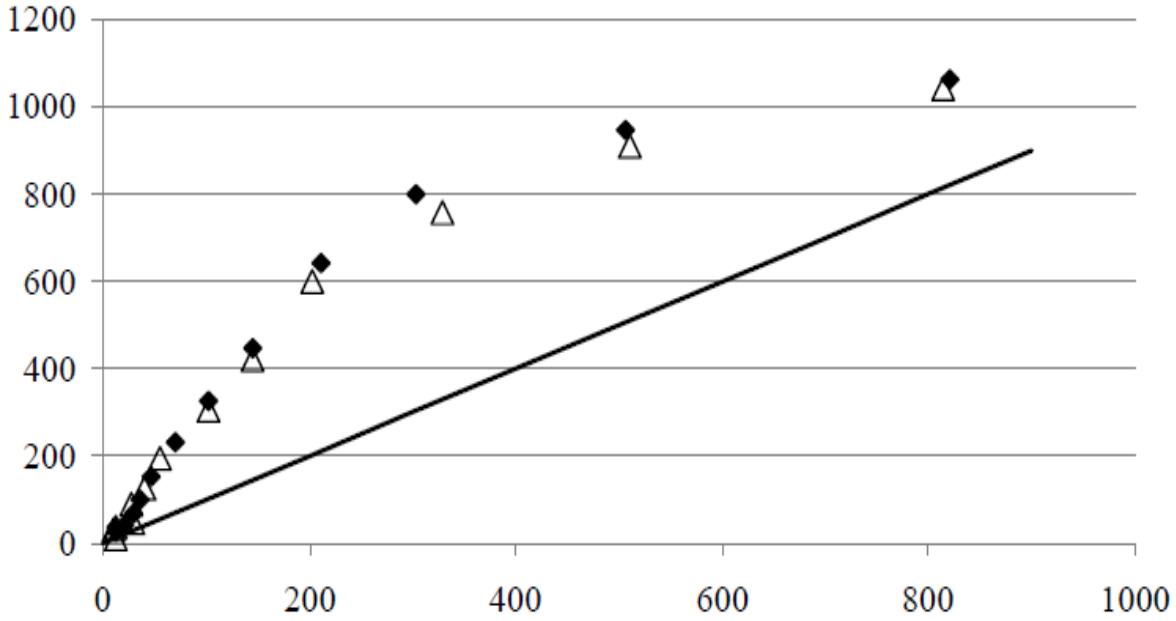


Figure 2. Relationship between the annual-mean total duration of extratropical cyclones $(N\tau)_c$ (ordinate) and anticyclones $(N\tau)_{ac}$ (abscissa) with different life times obtained from reanalysis data for two periods: 1948-1977 (Δ) and 1983-2012 (♦). Straight line corresponds to the equality of $(N\tau)_c$ and $(N\tau)_{ac}$.

According to Fig. 2 the relationship of $(N\tau)_c$ and $(N\tau)_{ac}$ is nonlinear. The cyclone-anticyclone asymmetry for the frequency of cyclones and anticyclones is the most pronounced for vortices with intermediate values of frequency or total duration.

## References

Akperov M.G., M.Yu. Bardin, E.M. Volodin, G.S. Golitsyn and I.I. Mokhov, 2007: Probability distributions for cyclones and anticyclones from the NCEP/NCAR reanalysis data and the INM RAS climate model. *Izvestiya, Atmos. Oceanic Phys.*, **43**(6), 705-712.

Akperov M.G. and I.I. Mokhov, 2013: Estimates of the sensitivity of cyclonic activity in the troposphere of extratropical latitudes to changes in the temperature regime. *Izvestiya, Atmos. Oceanic Phys.*, **49**(2), 113-120.

Mokhov I.I., O.I. Mokhov, V.K. Petukhov, and R.R. Khairullin, 1992: Effect of global climatic changes on the cyclonic activity in the atmosphere. *Izvestiya, Atmos. Oceanic Phys.*, **28**(1), 7-18.

# ATMOSPHERIC BLOCKINGS IN NORTHERN HEMISPHERE: VARIATIONS DURING LAST DECADES

I.I. Mokhov and A.A. Timazhev

A.M. Obukhov Institute of Atmospheric Physics RAS, Moscow, Russia
mokhov@ifaran.ru

Strongest regional weather-climate anomalies (including hot weather in summer and cold weather in winter) are related with the formation of long-lived blocking anticyclones (blockings). We analyze here variations of blocking activity in the Northern Hemisphere with the use of data from (http://solberg.snr.missouri.edu/gcc) for the period 1969-2013 (Wiedenmann et al., 2002; Mokhov et al., 2012).

Figure 1 shows seasonal longitudinal distributions for the blockings frequency in the Northern Hemisphere for two periods: 1969-1990 (I) and 1992-2013 (II). Significant increase in blocking frequency is noted during last decades according to Fig. 1 for different seasons.

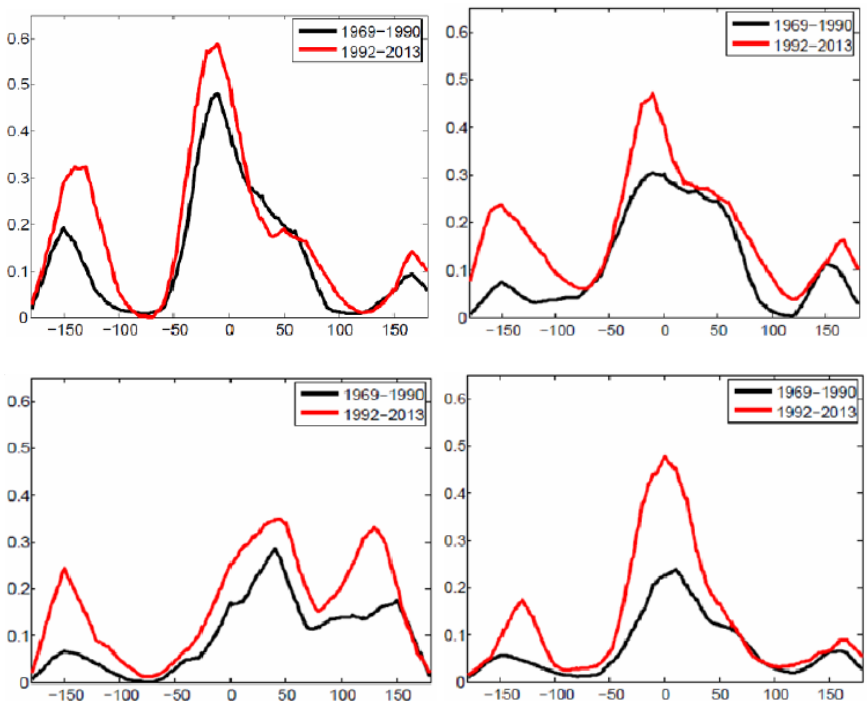


Figure 1. Longitudinal distributions for the blockings frequency in the Northern Hemisphere for two periods (1969-1990 and 1992-2013) in different seasons: winter (first row, first column), spring (first row, second column), summer (second row, first column), fall (second row, second column)/

We analyzed also the blockings frequency dependence on El-Nino/La-Nina phenomena (Mokhov, 2011). In particular, different transitions were analyzed similar to (Mokhov and Timazhev, 2013). Figure 2 shows longitudinal distributions of blockings frequency in summer for years in the neutral El-Nino/La-Nina phase (N) at the beginning (like 2014) and in the El-Nino phase (E) or neutral one at the end of the year. According to the forecasts these two

transitions (N→E and N→N) are the most probable for the year 2014, especially transition N→E.

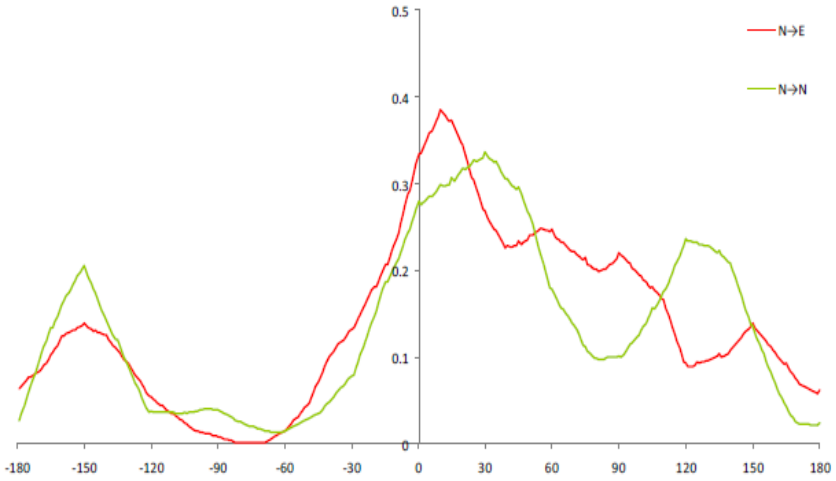


Figure2. Longitudinal distributions of blockings frequency in summer for years in the neutral El-Nino/La-Nina phase (N) at the beginning and in the El-Nino phase (E) or neutral one at the end of the year.

According to Fig. 2 the largest blockings frequency is corresponding for Western Europe for the most probable in 2014 transition N→E. That means high probability of blocking situation in summer 2014 for Western Europe with a high risk of summer heat wave.

The transition N→N is characterized by significant increase in the blocking frequency over Pacific Ocean. Such a regime was realized in summer 2013 with the long-lived blocking over Pacific. It was a key cause for the formation of the extreme flood in the Amur River basin in summer-fall 2013.

The Russian heat wave in summer 2010 due to long-lived blocking was corresponding to the E→L transition from El-Nino to La-Nina phase. The E→L transition is characterized by the highest risk of hot weather with drought conditions for European part of Russia according to (Mokhov and Timazhev, 2013).

## References

Mokhov I.I., 2011: Specific features of the 2010 summer heat formation in the European territory of Russia in the context of general climate changes and climate anomalies. *Izvestiya, Atmos. Oceanic Phys.*, **47**(6), 653-660.

Mokhov I.I., M.G. Akperov, M.A. Prokofyeva, A.V. Timazhev, A.R. Lupo and H. Le Treut, 2013: Blockings in the Northern Hemisphere and Euro-Atlantic Region: Estimates of changes from reanalysis data and model simulations. Doklady Earth Sci., **449**(2), 430-433.

Mokhov I.I. and A.V. Timazhev, 2013: Climatic anomalies in Eurasia from El-Nino/La-Nina effects. Doklady Earth Sci., **453**(1), 1141-1144.

Wiedenmann J.M., A.R. Lupo, I.I. Mokhov and E.A. Tikhonova, 2002: The climatology of blocking anticyclones for the Northern and Southern Hemispheres: Block intensity as a diagnostic. *J. Climate*, **15**(23), 3459–3473.

# Application of the ERA-Interim reanalysis to the energetics of a subtropical 'hybrid' low

Alexandre B. Pezza[1], Luke Garde[2] and Ian Simmonds[1]

[1]School of Earth Sciences, The University of Melbourne, Victoria, 3010, Australia
[2]Bureau of Meteorology, Melbourne, Victoria 3001, Australia
apezza@unimelb.edu.au

We have examined, with the ERA-Interim reanalysis dataset, new aspects of the genesis and partial tropical transition of a rare hybrid subtropical cyclone on the eastern Australian coast. The genesis mechanisms of 'Duck' (March 2001) were remarkably similar to the first South Atlantic hurricane (March 2004) (Pezza and Simmonds 2005). Lorenz energetics (Lorenz 1967) have been used in a number of analyses of intense cyclonic systems (e.g., Veiga et al. 2008, Pezza et al. 2010), and the approach is proving to be of immense value. We report here on an investigation which uses the Lorenz energetics method to diagnose the evolution of Duck.

Figure 1 shows the brightness temperatures in the developing phase of 'Duck' (at 0132 UTC 7 March 2001) just prior to the time it made its landfall. The image conveys the intensity of the system as well as the complex environmental conditions in which it was situated. Duck was a rare westward-propagating low which had a hybrid thermal structure partially driven by upper level baroclinicity and partially driven by tropical processes in association with strong surface heat fluxes. A broad range of properties of Duck were calculated during its lifetime using the cyclone tracking scheme of Simmonds and Rudeva (2012).

The environmental energetics analysis we have performed shows it was associated with a sharp barotropic conversion maxima just prior to the genesis, while a weaker peak occurred at the time the system first acquired an upper level warm core. The landfall was coincident with baroclinic conversions associated with thermal dissipation inland. Overall, the conversions during the developing phase were modest and not exclusively barotropic, explaining why the cyclone did not attain hurricane status although it had formed under similar conditions as the South Atlantic hurricane Catarina. The energetic analyses we undertook were conducted over multiple domains, and each revealed special insights into the relative influence of the various forcings. More details of these analyses can be found in Pezza et al. (2014).

## *References*

Lorenz, E. N., 1967: The nature and theory of the general circulation of the atmosphere. WMO Publ. No. 218, 161 pp.

Pezza, A. B., L. A. Garde, J. A. P. Veiga and I. Simmonds, 2014: Large scale features and energetics of the hybrid subtropical low 'Duck' over the Tasman Sea. *Climate Dyn.*, **42**, 453-466, doi: 10.1007/s00382-013-1688-x.

Pezza, A. B., and I. Simmonds, 2005: The first South Atlantic hurricane: Unprecedented blocking, low shear and climate change. *Geophys. Res. Lett.*, **32**, L15712, doi: 10.1029/2005GL023390.

Pezza, A. B., J. A. P. Veiga, I. Simmonds, K. Keay and M. d. S. Mesquita, 2010: Environmental energetics of an exceptional high-latitude storm. *Atmos. Sci. Lett.*, **11**, 39-45.

Simmonds, I., and I. Rudeva, 2012: The Great Arctic Cyclone of August 2012. *Geophys. Res. Lett.*, **39**, L23709, doi: 10.1029/2012GL054259.

Veiga, J. A. P., A. B. Pezza, I. Simmonds and P. L. Silva Dias, 2008: An analysis of the environmental energetics associated with the transition of the first South Atlantic hurricane. *Geophys. Res. Lett.*, **35**, L15806, doi:10.1029/2008GL034511.

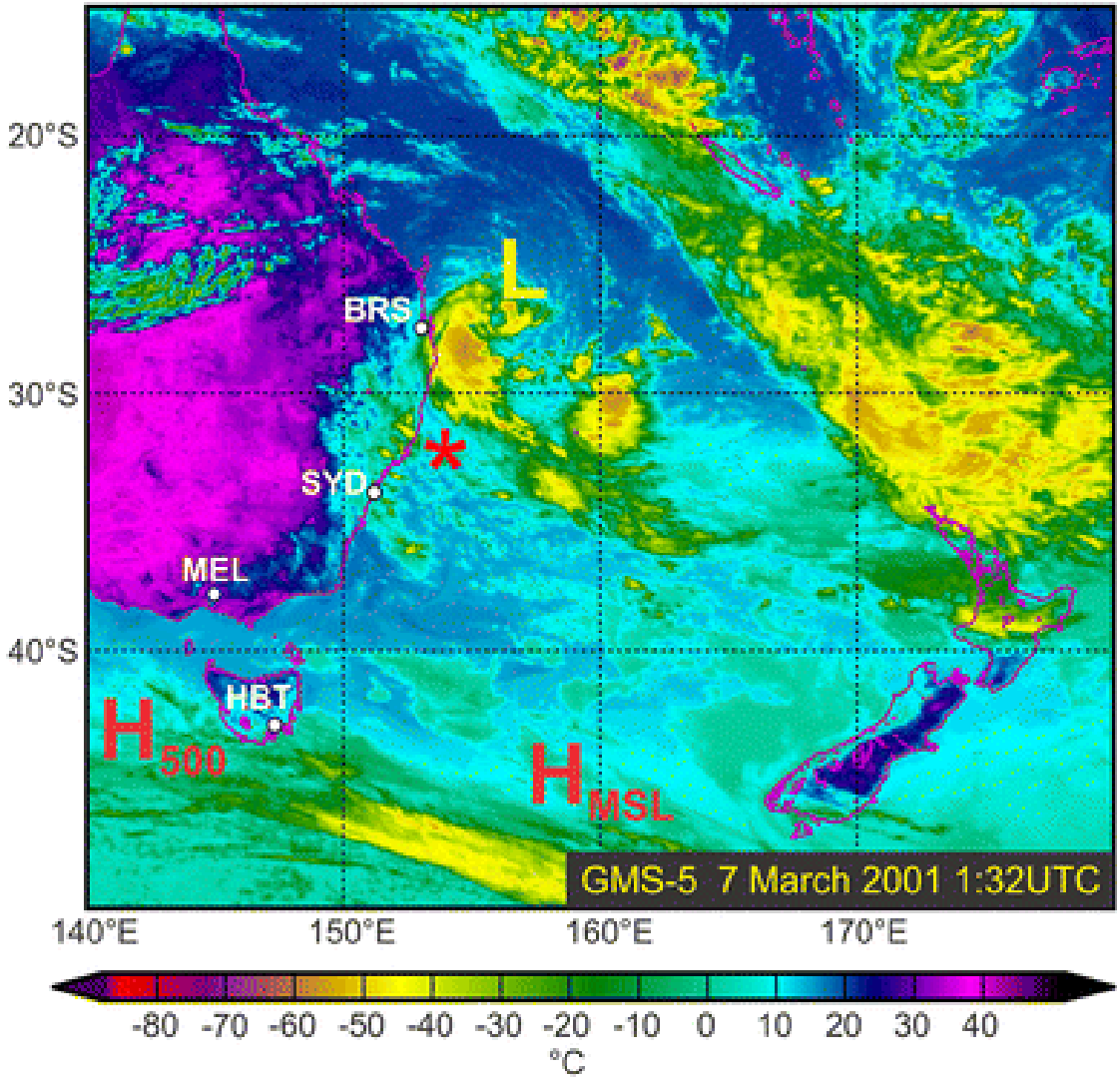


**Figure 1:** Brightness temperatures from GMS-5 image (over eastern Australia and the Tasman Sea) in the developing phase of 'Duck' (indicated with a yellow 'L') prior to landfall at 0132 UTC 7 March 2001.

# Changes in the Southern Hemisphere atmospheric circulation in recent decades

Ian Simmonds and Pallavi Govekar

School of Earth Sciences, The University of Melbourne, Victoria, 3010, Australia
simmonds@unimelb.edu.au

The circulation of the southern extratropics is very complex and varies according to a very broad scale of modes (e.g., Simmonds 2003, Simmonds and King 2004). The mode which explains most temporal variability is the Southern Annular Mode (SAM) (e.g., Marshall 2003), and the SAM is intimately tied up with transient eddies through complex wave-mean flow interactions (e.g., Rashid and Simmonds 2004, 2005). It has been suggested that trends in the SAM are associated with the increase in extent of Antarctic sea ice.

Over the period 1979-2013 the SAM has exhibited significant positive trends in summer (December – February) ($p < 0.05$) and autumn (March – May) ($p < 0.10$), but not in the other two seasons (Simmonds 2014). We here show the trends in the sea level pressure (SLP) over the southern extratropics calculated from the ERA-Interim reanalysis for the period 1979-2013. Fig. 1 shows, as expected, a very SAM-like signal in the summer pressure trends. In autumn similar significant shifts in the meridional SLP distribution may be seen in the Pacific, whereas an opposite signal is see in the Atlantic and there are strong positive trends to the east of the Weddell Sea. In winter and spring one can appreciate from the Figure that there is little trend in the zonal means, but spring does show a significant increase between about 50 and 60$^{o}$S to the northeast of the Weddell Sea. It will be noted that the pattern in spring resembles the Pacific-South American teleconnection pattern.

## *References*

Marshall, G. J., 2003: Trends in the southern annular mode from observations and reanalyses. *J. Climate*, **16**, 4134-4143.

Rashid, H. A., and I. Simmonds, 2004: Eddy-zonal flow interactions associated with the Southern Hemisphere annular mode: Results from NCEP-DOE reanalysis and a quasi-linear model. *J. Atmos. Sci.*, **61**, 873-888.

Rashid, H. A., and I. Simmonds, 2005: Southern Hemisphere annular mode variability and the role of optimal nonmodal growth. *J. Atmos. Sci.*, **62**, 1947-1961.

Simmonds, I., 2003: Modes of atmospheric variability over the Southern Ocean. *J. Geophys. Res.*, **108**, 8078, doi: 10.1029/2000JC000542.

Simmonds, I., 2014: Comparing and contrasting the behaviour of Arctic and Antarctic sea ice over the 35-year period 1979-2013. *Ann. Glaciol.*, (in press).

Simmonds, I., and J. C. King, 2004: Global and hemispheric climate variations affecting the Southern Ocean. *Antarc. Sci.*, **16**, 401-413.

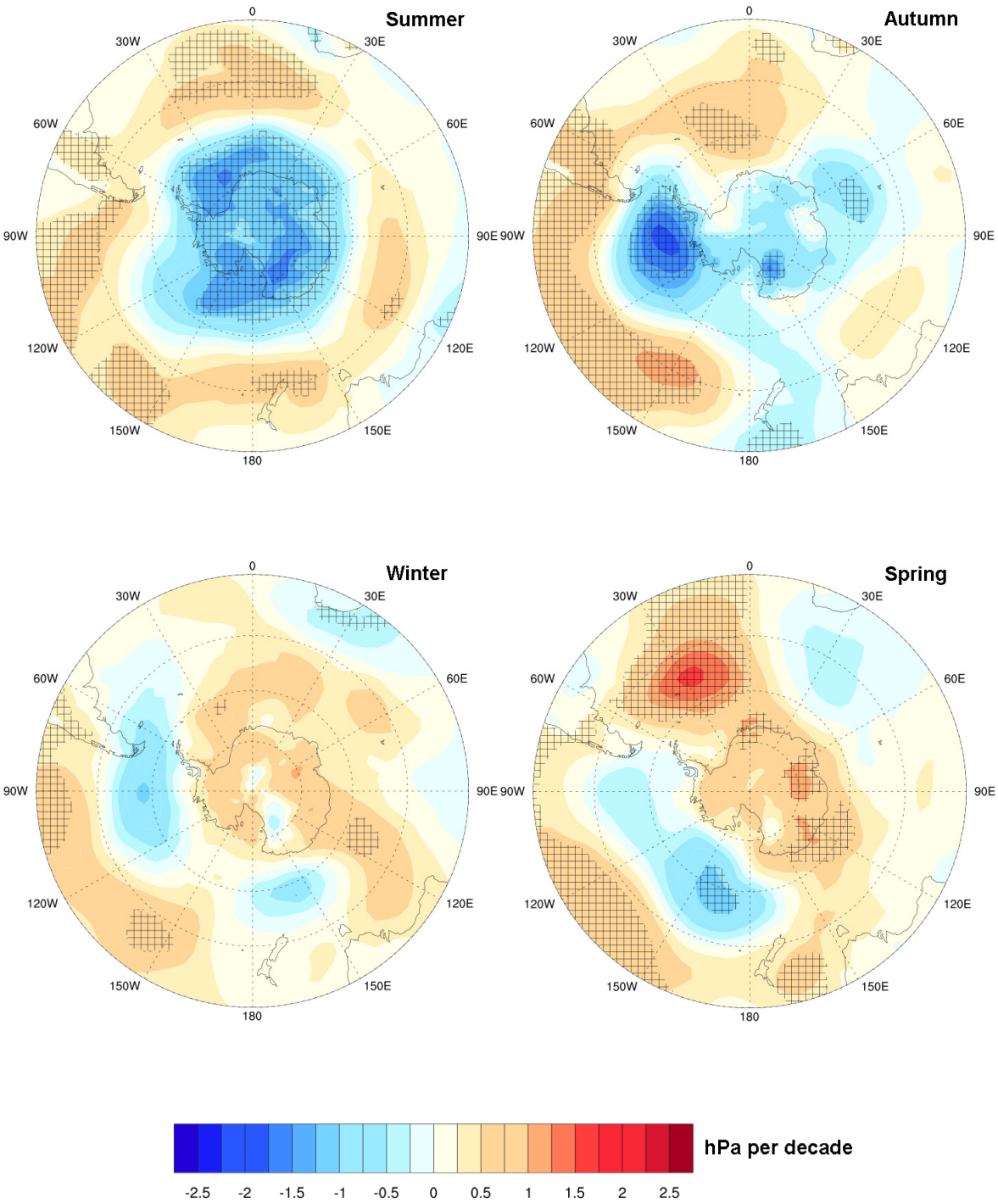


**Fig. 1:** SH extratropical SLP trends (1979 to 2013) for Summer, Autumn, Winter, and Spring for the period. The units are hPa per decade, and cross hatching denotes regions over which the trends differ significantly from zero at the 90% confidence level.

# Data Impacts on QPF Verification: A Comparison of the CCPA with StageIV for Heavy Precipitation Events in the HMT-West

*Edward Tollerud[1,3], John Halley Gotway[2,3], Tressa Fowler[2,3], Tara Jensen[2,3], and Barbara Brown[2,3]*

*[1]Cooperative Institute for Research in the Atmosphere, Fort Collins, CO*

*[2]National Center for Atmospheric Research, Boulder, CO*

*[3]Developmental Testbed Center, Boulder, CO*

## 1. Introduction

NCEP/EMC in collaboration with CPC has recently developed a new QPE product called the Climate Corrected Precipitation Analysis (CCPA; Hou *et al.*, 2012). The motivation for the CCPA was to design a QPE product at a finer scale than the available CPC gage analysis that retained the statistical properties of the original CPC analysis. Since this new product is significantly based on the existing Stage IV product, the question is raised: is it a suitable replacement for Stage IV that can be used for weather-related operational verification? For the HMT-West verification project, which has used Stage IV as one of its verification datasets for its winter exercise verification studies, the issue is one of year-to-year consistency as well as one of potential value added by the CCPA. Hou *et al.* (2012) address differences between the CCPA and Stage IV using full-CONUS accumulated precipitation, concluding that the CCPA under-estimates the heavier precipitation totals. For the present evaluation, we have concentrated on 6h totals and on the smaller HMT forecast domain in California during several heavy rain episodes during the winters of 2009-10 and 2010-11. The primary emphasis here reflects an objective of the HMT winter exercises in California, which was to evaluate the impact of the choice of QPE analyses on model verification scores during episodes of heavy and extreme precipitation.

## 2. Results

Fig. 1 shows a direct comparison between the two analyses as given by a verification score (frequency bias) that here uses Stage IV as the verification 'observation set' and the CCPA as the verification 'target' (more typically a numerical forecast). Scores are computed over the HMT domain during winters between 2005 and 2011, and for 6h values of both Stage IV and CCPA. It is clear from the figure that the CCPA (relative to the Stage IV) very slightly over-forecasts at the smallest thresholds, but significantly under-forecasts the larger amounts, a finding consistent with that of Hou *et al.* (2012). For actual model verification (now for heavy rainfall episodes during 2009-2011, also within the HMT domain), Fig. 2 illustrates the impact of using the CCPA and the Stage IV as verification analyses for model predictions. At the heavier rainfall thresholds in particular, scores of the GSS are consistently better when the QPE estimates used are those produced by Stage IV, whereas for frequency bias the CCPA produce better scores. A likely source for these differences is the apparent under-estimate (and smoothing out) of heavier precipitation events by the CCPA suggested by Fig. 1. Based on these findings, we suggest careful reliance on verification studies for heavy precipitation that compare or combine results from these two analyses.

*References*

Hou, D., M. Charles, Y. Luo, Z. Toth, Y. Zhu, R. Krzysztofowicz, Y. Lin, P. Xie, D.-J. Seo, M. Pena, and B. Cui, 2012: Climatology-Calibrated Precipitation Analysis at Fine Scales: Statistical Adjustment of Stage IV towards CPC Gauge Based Analysis. *J. Hydrometeor*. doi:10.1175/JHM-D-11-0140.1, in press.

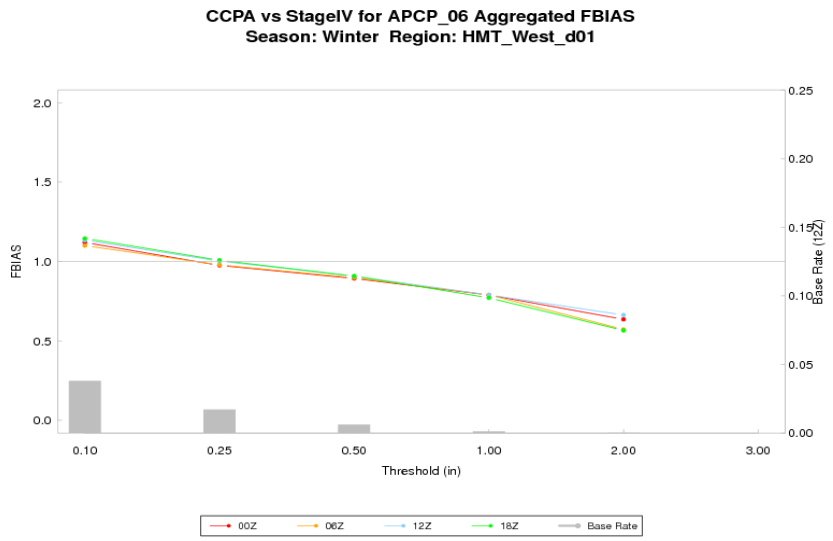


Fig. 1. Frequency bias for the CCPA relative to the Stage IV over the HMT domain for winters between 2005 and 2011 at several thresholds and 4 model valid times.

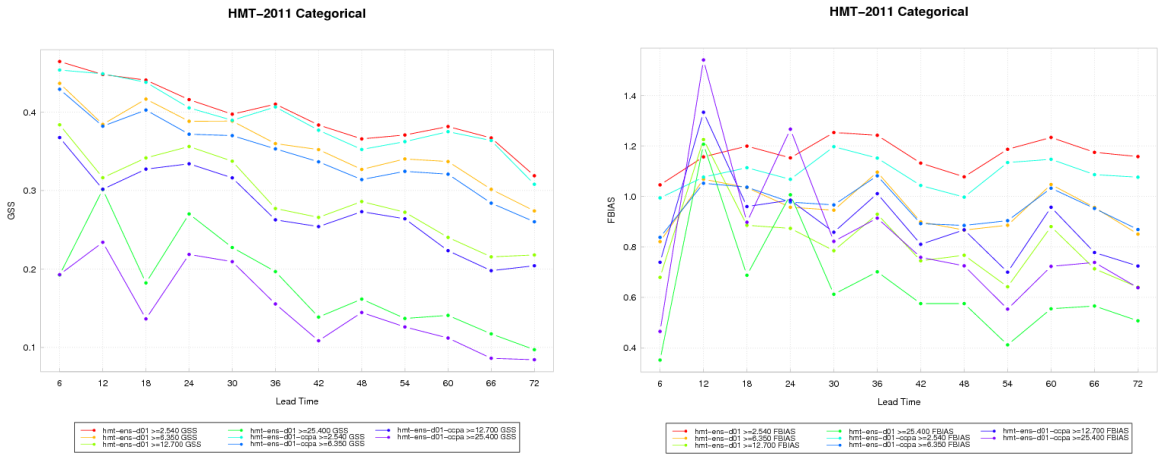


Fig. 2. Comparison of Stage IV- based and CCPA-based Gilbert skill scores (or equitable threat scores, left panel; larger values better) and frequency bias (right panel; values near 1 better) over the HMT domain for all ensemble mean forecasts at lead times and precipitation thresholds as shown. Line colors to be paired can be determined from the legends; generally, blue colors are CCPA-based and others are Stage IV-based.

# Potential vorticity thinking in convective storms forecasting

Yury I. Yusupov
MapMakers Group Ltd., Moscow, Russia. E-mail: usupov@gismeteo.com

Potential vorticity thinking is widely used in understanding of atmospheric dynamics and the evolution of large-scale weather systems. In this paper an attempt to use this conception for mesoscale weather phenomena forecasting is presented.

Hazardous weather events - large hail, damaging wind gusts, heavy rainfall and in some cases tornados produced by deep, moist convection are called convective storms. According to the present-day conception, three conditions are needed for the deep moist convection (Doswell and Bosart, 2000):

—the humidity in the surface layer is not lower than 60%;
—the instability or weak stability in the lower troposphere;
—the dynamic forcing; as a result, air particles are lifted up to the free convection level.

It is known that the majority of active convective zones are formed on the cold fronts. One of the conditions for the existence of active frontal zones is the sufficient amount of moisture in the surface layer. The convective unstable or weak-stable layers are systematically formed in the vicinity of fronts. Thus, the first two of the three conditions needed for the development of the deep moist convection are met in the active frontal zone. The third condition is the dynamic forcing that causes the lift of the air particles to the free convection level. In (Hoskins et al, 1985), the explosive pressure drop on the Earth's surface is explained by the intense upward motions formed in the area of intersection of the positive (in the Northern Hemisphere) anomaly of potential vorticity with the baroclinic zones in the lower troposphere. A system with the positive feedback is formed as a result of this interaction which consists of the potential vorticity anomaly in the upper atmospheric layers and positive temperature anomaly in the surface baroclinic zone. Thus, on the one hand, the existence of the positive anomaly of *PV* in the troposphere is a sign of the existence of active convection zones (Russell et al, 2012) and, on the other hand, the interaction between the *PV* anomaly and the surface baroclinic zones forms the conditions for the dynamic forcing that favors the formation and intensification of convection. Hence, having determined the anomalies of potential vorticity and surface baroclinic zones under condition of their intersection, the existence or formation of the active convection zone in this area can be supposed with high probability. According to (Peskov and Snitkovskii, 1968), in the case of the squall the wind speed depends on the kinetic energy of the downward flow in the cumulonimbus cloud and under it, and on the speed of the horizontal wind in lower and middle tropospheric layers. Therefore, it is necessary to study the vertical distribution of the wind in the revealed area because squalls are formed as a result of air sinking and transfer of momentum in the downward direction. The traditional approach to forecasting deep moist convective zones is definition of convective instability with the help of CAPE calculation and various instability indexes such as K-index, Lifted index, Total-totals index etc. This approach has one serious disadvantage: it works only in warm period of the year, when convection occurs mostly due to convective (static) instability. During the cold season this type of instability is observed much more seldom. In winter most of convective phenomena are associated with the conditional symmetric instability (Reuter and Aktary, 1995). Unlike the traditional methods of active convective zones forecasting, the approach suggested in present paper is not directly related to instability type definition. Therefore, this method is expected to work equally effective in warm and cold periods of the year.

The algorithm suggested (Yusupov, 2013):

1. Active convection zones are defined by finding intersection of PV anomalies and surface baroclinic zones. The baroclinic zones are calculating by Huber-Pock and Kress method (Huber-Pock and Kress, 1989).

2. In the found zones maximum gusts of wind are calculating by empirical formulae by Peskov and Snitkovskii method (Peskov and Snitkovskii, 1968).

Fig a): The situation on July 30, 2010, 06:00 UTC. Input data – forecast for 18 hours, 1.25x1.25 degrees, Exeter. MSL isolines (magenta) and calculating frontal lines are shown. Blue dash lines – baroclinic zones, red lines – areas when PV≥0.6 PVU; brown dash lines indicate areas of intersection of PV anomalies and low level baroclinic zones; yellow-red shading – zones where forecasting gusts of wind ≥20 m/s. Signs of wind – gusts of wind according to observation data, black digits – forecasting gusts of wind.

Fig b): The situation on December 13, 2013, 12:00 UTC. Input data – forecast for 12 hours, 1.25x1.25 degrees, Exeter. MSL isolines and calculating frontal lines are shown. Yellow-red shading –zones where forecasting gusts of wind ≥20 m/s. Signs of wind – gusts of wind according to observation data, black digits – forecasting gusts of wind.

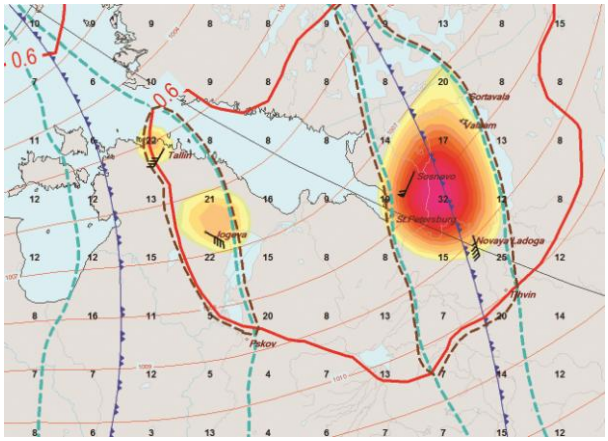


a) Convective storms forecasting on July, 30, 2010, 06:00 UTC

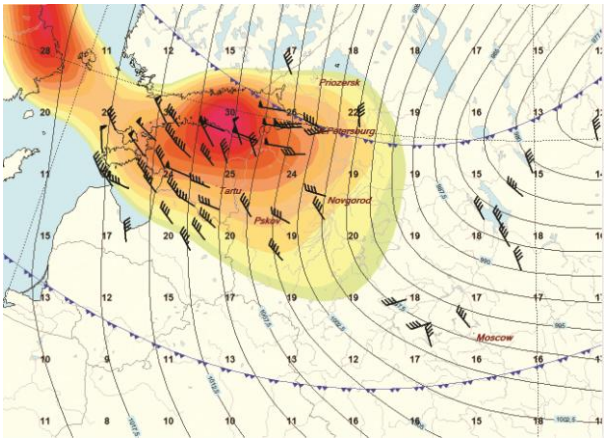


b) Convective storms forecasting on December, 13, 2013, 12:00 UTC

## References


**Doswell C. A. and L. F. Bosart L. F**., *Extratropical Synoptic-scale Processes and Severe Convection. A Meteorological Monograph* (Amer. Meteorol. Soc., 2000).

**Hoskins B. J., McIntyre M. E., and Robertson A. W**. On the Use and Significance of Isentropic Potential Vorticity Maps, Quart. J. Roy. Meteorol. Soc., 1985, vol. 111, No. 470, pp.877 – 946.

**Huber-Pock F. and Kress Ch**. An operational model of objective frontal analysis based on ECMWF products. – Meteorol. Atmos. Phys., 1989, vol. 40, № 2, pp. 170 – 180.

**Peskov B. E. and Snitkovskii A. I.**, On the Forecast of Severe Squalls. – Russian Meteorology and Hydrology, 1968, № 7.

**Reuter G. W. and Aktary N.** Convective and symmetric instabilities and their effect on precipitation: Variation in Central Alberta during 1990 and 1991. – Mont. Wea. Rev., 1995, vol. 16, pp. 153 - 161.

**Russell A., Vaughan G. and Norton E. G.** Large-scale potential vorticity anomalies and deep convection. – Quart. J. R. Meteorol. Soc., 2012, vol. 138, pp. 1627 - 1639.

**Yusupov Yu. I.** Squall forecast method using thermodynamic atmospheric parameters and Ertel's potential vorticity. – Russian Meteorology and Hydrology, 2013, vol. 38, Issue 11, pp.759 – 765.